Nguyen, H. B. K. *et al.* (2024). *Géotechnique* **74**, No. 12, 1503–1508 [https://doi.org/10.1680/jgeot.20.D.005]

DISCUSSION

How particle shape affects the critical state, triggering of instability and dilatancy of granular materials – results from a DEM study

H. B. K. NGUYEN*, M. M. RAHMAN†, A. B. FOURIE‡, X. D. LUO§, X. TANG§ and J. YANG§

Contribution by X. D. Luo, X. Tang and J. Yang

How particle shape plays a role in the overall mechanical behaviour of granular soils is a fundamentally important question and has been the focus of the discussion contributors' research endeavours over the years (e.g. Yang & Wei, 2012; Wei & Yang, 2014; Yang & Luo, 2015; Liu & Yang, 2018). In particular, Yang & Luo (2015) presented results from specifically designed experiments to explore the relationship between critical state and particle shape, in which the effect of particle shape was carefully isolated from other influencing factors, such as particle size, gradation and minerology. The authors of the paper (Nguyen *et al.*, 2021: p. 750) appeared to be unaware of these studies in stating that 'to study the effect of particle shape on the mechanical behaviour of soils that have the same grain size distribution and mineralogy…is almost unachievable experimentally'. In this short discussion contribution, the discussers would like to share some experimental results for the purpose of evaluating the numerical results in the paper. Interested readers can refer to the aforementioned publications for more detailed results and discussion.

CRITICAL STATE PARAMETERS

Based on the experimental data of Yang & Luo (2015), the following expressions can be established relating the critical state parameters (M, e_Γ, λ_c) of a uniformly graded granular material to its overall shape parameter (OR)

$$M = 4{\cdot}67 - -3{\cdot}98\text{OR}$$

$$e_\Gamma = 0{\cdot}614(\text{OR})^{-2{\cdot}34}$$

$$\lambda_c = 0{\cdot}001(\text{OR})^{-21{\cdot}4}$$

where OR is referred to as overall regularity, collectively accounting for the sphericity, aspect ratio and convexity of the constituent particles. For a granular material composed of perfectly spherical particles, its OR value is 1, whereas for a fine sand with subangular to subrounded grains, its OR value is typically between 0·85 and 0·87 (Yang & Luo, 2015; Liu & Yang, 2018). Note that e_Γ and λ_c are the intercept and the gradient, respectively, of the critical state line (CSL) in the e–$(p'/p_a)^\xi$ plane, and they correspond to $e_{\lim}$ and Λ, respectively, in the paper under discussion. Also note that ξ is a non-sensitive parameter with a typical range between 0·6 and 0·7. The parameter M is the familiar stress ratio describing the slope of the CSL in the q–p' plane.

The above relationships give a consistent trend that the critical state parameters decrease with increasing particle regularity. This means that, other things being the same, the CSL of a granular soil with rounded particles is positioned lower and is less steep in both the q–p' plane and e–$(p'/p_a)^\xi$ plane compared with the CSL of a granular material with angular particles, as schematically shown in Fig. 15. For an assembly of perfectly spherical particles (OR = 1) – an idealised case frequently adopted in discrete-element method (DEM) simulations – the critical state parameters are estimated as follows: $M = 0{\cdot}69$, $e_\Gamma = 0{\cdot}614$, $\lambda_c = 0{\cdot}001$. Comparing these values with those obtained by the authors (Table 4): $M = 0{\cdot}80$, $e_\Gamma = 0{\cdot}68$, $\lambda_c = 0{\cdot}026$, one can readily notice the discrepancies.

In particular, the authors' value of λ_c (i.e. Λ) is one order of magnitude greater than the discussers' experimental prediction, and is comparable to that of uniform sands with subrounded to subangular grains (e.g. Toyoura sand and Fujian sand; see Verdugo & Ishihara (1996) and Yang & Wei (2012)). Such a large λ_c value is not considered possible for an assembly of uniform spheres. Furthermore, the simulation result shown in Fig. 9 of the paper – that λ_c (i.e. Λ) increases with increasing particle sphericity – is also in contrast with the experimental observation. Generally, a granular material with angular particles is more compressible than a granular material with rounded particles under otherwise similar conditions.

As far as the DEM simulations are concerned, one needs to be cautious in that these simulations can be greatly affected by various factors – such as contact models and parameters, specimen dimensions and number of particles, boundary treatment, and the loading/straining rate used. The way to properly model particle shape and determine critical states brings additional difficulty and uncertainty. To make the point, Fig. 16 here shows the CSL obtained for assemblies of uniformly graded spheres ($C_u = 1{\cdot}27$, $D_{50} = 1{\cdot}0$ mm) using three-dimensional (3D) DEM simulations (Tang & Yang, 2019). In the simulations, the Hertz–Mindlin (HM) model was adopted, with the values of Young's modulus and Poisson's ratio being similar to those of quartz grains. The gradient of the CSL in the compression plane (λ_χ) is quantified as 0·00084. Interestingly, this very small value is comparable to that obtained by Huang *et al.* (2014), also for uniformly graded spheres, 0·000923. Both studies suggest that the assemblies of uniform spheres have extremely low compressibility, as confirmed by the

*UniSa STEM, University of South Australia, Mawson Lakes, SA, Australia (Orcid:0000-0001-7280-9472).
†UniSa STEM, University of South Australia, Mawson Lakes, SA, Australia (Orcid:0000-0002-0638-4055).
‡School of Civil, Environmental & Mining Engineering, University of Western Australia, Crawley, WA, Australia (Orcid:0000-0001-7250-2104).
§Department of Civil Engineering, The University of Hong Kong, Hong Kong, P. R. China.

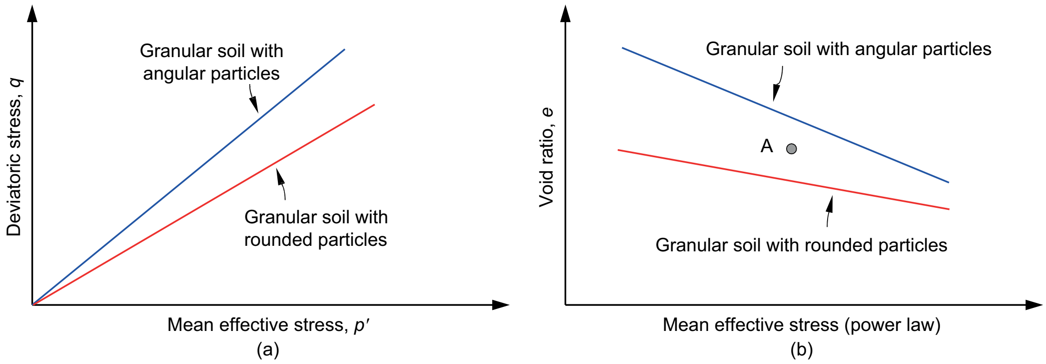

Fig. 15. Schematic illustrations of the effect of particle shape on the critical state locus in: (a) q–p' plane; (b) e–$(p'/pa)^{\xi}$ plane

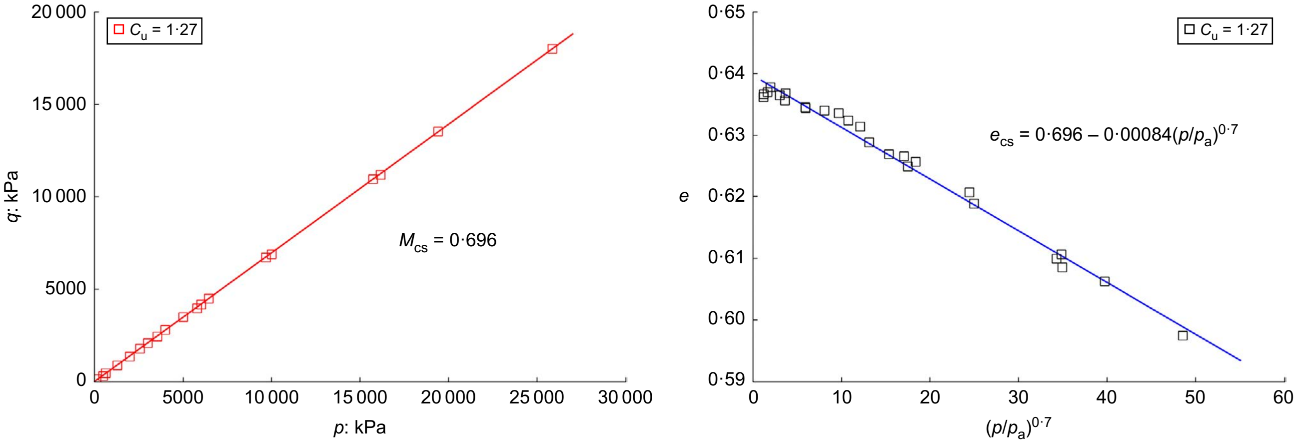

Fig. 16. Critical state locus of assemblies of uniform spheres from three-dimensional discrete-element method (3D DEM) simulations.

discussers' experimental data. Furthermore, the simulations of Tang & Yang (2019) give a value of 0·696 to the critical stress ratio M, which is in good agreement with the predicted value (0·69) using the relationship derived from the discussers' experiments. However, the authors' simulations give a significantly larger value of 0·8. The possible reasons for the discrepancy include the interparticle friction assumed in the DEM simulations and the criteria for the determination of the critical states.

TRIGGERING OF INSTABILITY

Based on experimental data and the critical state theory, Yang (2002) proposed an exponential function relating the slope of the instability line (η_{IS}) to the initial state parameter (ψ_0). While the simulation results in Fig. 10 of the paper exhibit this trend in general, the results do not appear to reflect the effect of particle shape correctly. The physically unsound features in Fig. 10 include: (*a*) the uniformly graded spheres have a resistance to the triggering of instability

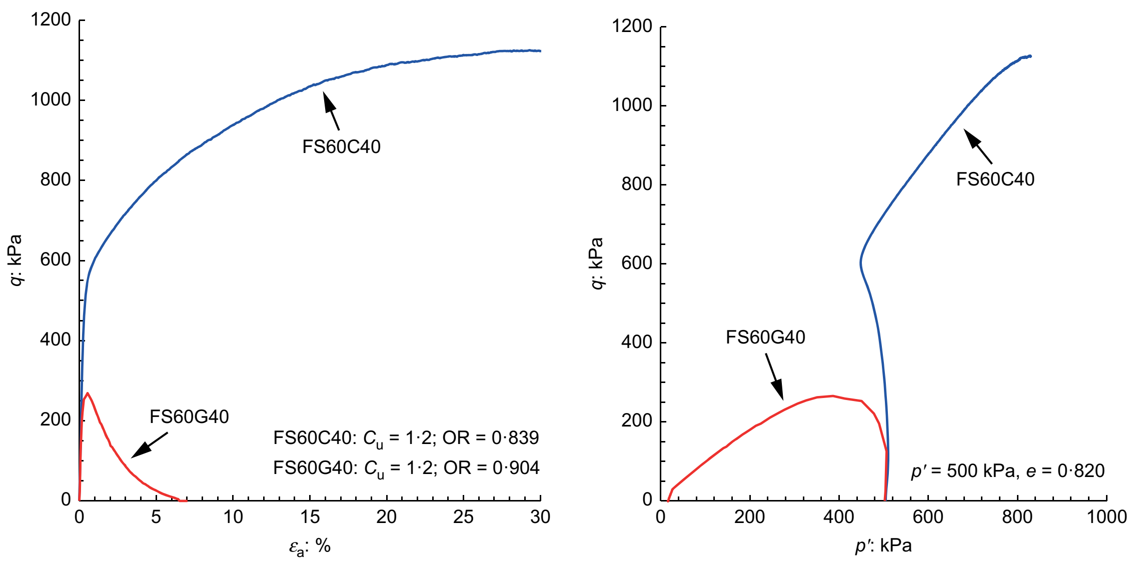

Fig. 17. Experimental evidence for effect of particle shape on the overall behaviour (data from Yang & Luo (2015))

comparable to that of natural sands with subangular to subrounded grains; (*b*) the uniformly graded spheres have much stronger resistance to the triggering of instability than the uniformly graded ellipsoids; (*c*) the trendlines for the two cases of cluster particles are positioned lowest, meaning that they are most susceptible to the triggering of instability. Some of these features are also inconsistent with the authors' own results in Table 4. For example, if the assemblies of ellipsoids have an M value greater than that of assemblies of spheres, then they should exhibit larger dilatancy and stronger resistance to instability according to the stress dilatancy theory (e.g. Wood *et al*., 1994; Yang & Li, 2004), but the data in Fig. 10(a) indicate the opposite.

As far as the effect of particle shape on the undrained instability is concerned, Yang & Luo (2015) reported clear evidence as shown in Fig. 17. The two specimens were consolidated to the same void ratio and mean confining stress and then subjected to the same undrained loading condition. One of the specimens (FS60G40) was composed of more rounded particles (OR = 0·904) and the other (FS60C40) composed of relatively angular particles (OR = 0·839), but both had identical C_u, D_{50} and mineralogy. The specimen FS60G40 underwent complete liquefaction, whereas the specimen FS60C40 exhibited strong dilatancy with no occurrence of instability. The observed behaviour can be well explained in the framework of critical state soil mechanics. Referring to Fig. 15, the CSL of a granular soil with rounded particles is positioned below the CSL of its counterpart with angular particles. For a given state (A) in terms of void ratio and mean effective stress, the state is then characterised as a loose state with reference to the CSL of the rounded granular soil, meaning that the expected behaviour is contractive and liquefaction-susceptible; whereas with reference to the CSL of the angular granular soil, the same initial state is characterised as a dense state and the behaviour is hence expected to be dilative and non-liquefiable.

Authors' reply

The authors thank the discussers for sharing opinions on their research using schematic diagrams and their experimental data. The authors used a numerical approach, the DEM, to evaluate the effect of particle shapes on qualitative triaxial loading behaviours – for example, critical state (CS), instability and dilatancy. This approach is different from simulating a known soil behaviour, but the authors had to adapt it, owing to the lack of real soils that have different particle shapes but are identical in all other factors which could affect mechanical behaviour. It is important to be careful in that experiments and numerical simulations both have certain advantages and limitations. Although the experimental work may provide direct evidence of the effect of particle shapes on the mechanical behaviour of real soils, the soil fabric – which is affected by the particle shapes and controls the overall mechanical behaviour – is mostly unknown. The authors' work also evaluates those micromechanical aspects.

All DEM simulations in this study had the same contact model, boundary (periodic) condition, number of particles, strain rate, preparation method, PSD and other model input parameters. The only difference was their particle shapes. In short, the granular materials in the authors' study have the same mineralogical behaviour and PSD, but with different particle shapes. The discussers also suggested that 'the effect of particle shape was carefully isolated from other influencing factors such as particle size, gradation and minerology' for Fujin sand, glass beads and crushed glass beads in the paper by Yang & Luo (2015) and compared with the authors' work. While their study is commendable for experimental work, the degree of isolation of these factors was not as high as in this DEM study. Table 5 only compares the uniformity coefficient, $C_u = D_{60}/D_{10}$ for PSD curves; D_{60} and D_{10} are particle sizes at 60 and 10% finer on the PSD curve. The maximum difference of C_u in the paper by Yang & Luo (2015) was 0·20, whereas it was only 0·02 in the paper by Nguyen *et al*. (2021). Therefore, the level of isolation of gradation effect was not as great as in the DEM.

The discussers raised concerns on the trend of CS parameters and the triggering of instability behaviour. The authors believe these were due to their adoption of traditional parametric values – for example $\xi = 0{\cdot}70$ – and practices for the critical state soil mechanics (CSSM) framework. This discussion provides the authors with an opportunity to clarify and develop a wider understanding.

CRITICAL STATE PARAMETERS

Nguyen *et al*. (2021) identified that one of the challenges in quantifying the influence of particle shape on mechanical behaviour is the lack of use of a common shape descriptor, and they deliberately used a very simple shape descriptor of sphericity (S) using a well-known chart (Krumbein & Sloss, 1963). Yang & Luo (2015) may be credited for developing correlations of CSL parameters and overall regularity (OR), which is intended to collectively account for S, aspect ratio and convexity of a particle. S and OR are not directly comparable, and the relations provided in the discussion are not directly comparable to the authors' study. However, since S and OR are 1 for a perfect sphere and if one assumes S increases as OR increases, then the qualitative trend of decreasing M and e_{lim} with S in the DEM and OR in the discussers' experimental data are similar. The reader must be aware that such comparison is only possible when the influence of aspect ratio and convexity are completely ignored in the shape descriptor.

The authors also noticed an intriguing difference in interpreting CS data, which partly led to the discussers' confusion. This will be explained here in detail for interested readers. Traditionally, the CSL was assumed as a straight line in e–ln (p') space and expressed as $e_{\text{CS}} = e_\Gamma - \ln(p')$. In the last two decades, it has been realised that the trend of the CS data points may be better presented by a curve in e–log (p') space, particularly at higher p'. Often a power function as $e = e_{\text{lim}} - \Lambda(p'/p_a)^\xi$ (Li & Wang, 1998), is adopted to present the CSL in the e–log (p') space. The best-fit trend line for the available CS data points is obtained by regressional analysis, which gives the values of e_{lim}, Λ and ξ. The best-fit trend has the utmost importance in the application of the

Table 5. PSD curve parameters

	Nguyen *et al*. (2021)		Yang & Luo (2015)		
	Sphere/cluster	Ellipsoid	Fujian	Glass bead	Crushed glass bead
Coefficient of uniformity, C_u	1·67	1·69	1·29	1·26	1·46

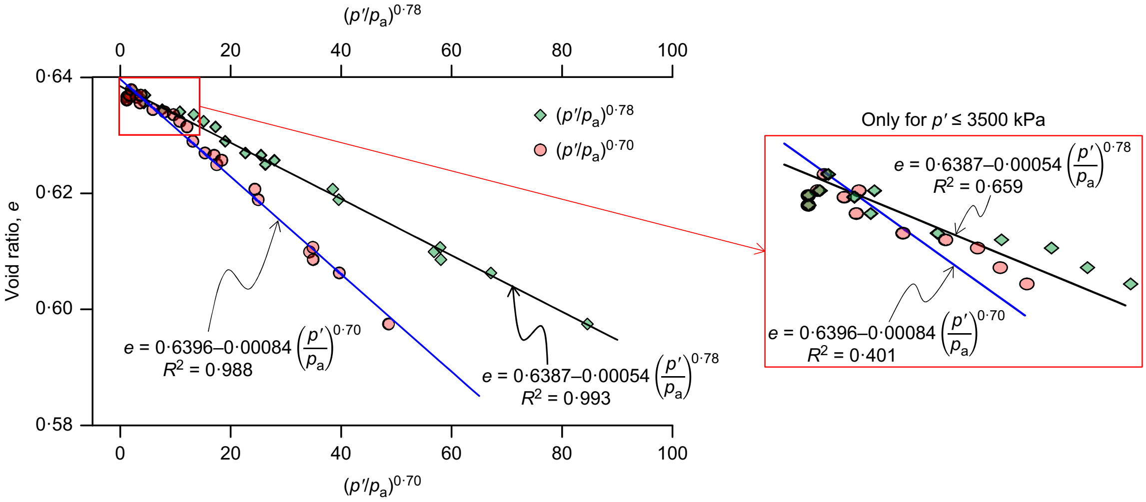

Fig. 18. Comparison of the slope of the trend lines for the best-fit ξ of 0·78 and a constant ξ of 0·70 for the same critical state (CS) data points in the e–$(p'/p_a)^{\xi}$ space

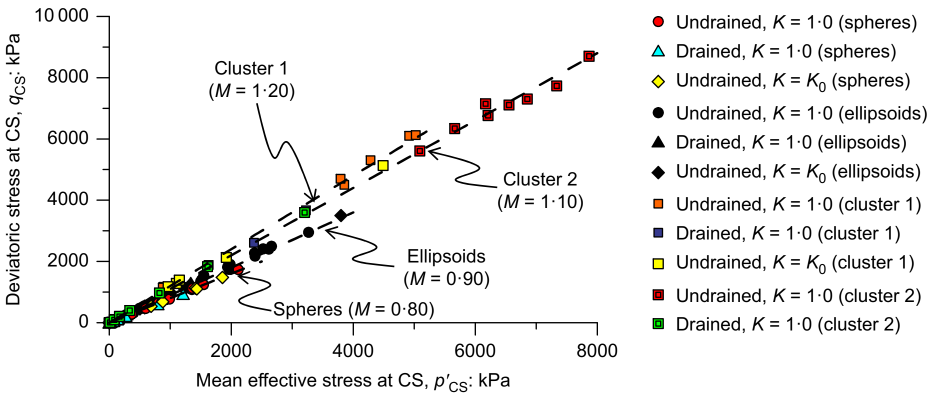

Fig. 19. Critical state lines (CSLs) for different particle shapes

CSSM framework – for example, a shift between CS data points and inferred CSL introduces a systematic error in the calculation of state parameters. Such error will certainly affect many state parameter-dependent correlations (Jefferies & Been, 2006; Rahman *et al*., 2011; Rabbi *et al*., 2019), cyclic liquefaction assessment (Rahman & Sitharam, 2020; Rahman *et al*., 2021) and constitutive modelling (Li & Dafalias, 2000; Rahman *et al*., 2014).

Knowing the best-fit trend is desirable, it should be noted that a power function does not have a gradient unless a value is pre-assumed for the parameter ξ and presented as a straight line in the e–$(p'/p_a)^{\xi}$ space. A recent round-robin programme on determining CSL in 15 different laboratories around the world showed that CSLs were in a narrow range in the e–$\log(p')$ space but ξ varied between 0·176 to 0·720 in conjunction with e_{lim} and Λ (Reid *et al*., 2021). Therefore, the authors tend to disagree with the discussers that ξ is 'a non-sensitive parameter', particularly assuming a constant ξ of 0·70 to define a gradient of the CSL. The authors re-analysed the discussers' DEM data with the best-fit $\xi = 0.78$ and compared with their analysis for $\xi = 0.70$ as shown in Fig. 18; $\xi = 0.78$ improved the correlation with a higher coefficient of determination (R^2) than $\xi = 0.70$. Noticeably, it also significantly changed the gradient of the CSL in e–$(p'/p_a)^{\xi}$ space, Λ (which the discussers refer to as λ_c or λ_χ). The authors also noticed that R^2 has a higher deviation for a low stress level for the same data. Therefore, a general perception of assuming a numeric value for any of the CSL parameters (for power function), particularly $\xi = 0.70$, is misleading, as then the slope of the trend lines would be different, even for the same CS data points (see Fig. 18). This suggests that the qualitative trend for the gradient of CSL in the schematic diagram in Fig. 16 provided by the discussers is only comparable when two soils have the same ξ, but this should not be the case.

However, the CSL in q–p' space did not have such an interpretation issue, and the authors agree with the discussers' schematic diagram in Fig. 16 that the slope of the CSL (M) reduces with sphericity (S) of the particles, as shown in Fig. 19.

The discussers also identified that Λ and M values were higher in the current study compared to extracted DEM data

Table 6. The differences in the DEM models

	Nguyen *et al.* (2021)	Huang *et al.* (2014)
Method	Qualitative	Calibrate Toyoura sand
Particle size	m	mm
PSD parameter, C_u	1·67	1·386
PSD parameter, C_c	0·998	0·977
Contact model	Linear	Hertz–Mindlin
Coefficient of friction	0·5	0·25

Note: the report by Tang & Yang (2019) was not available to the authors.

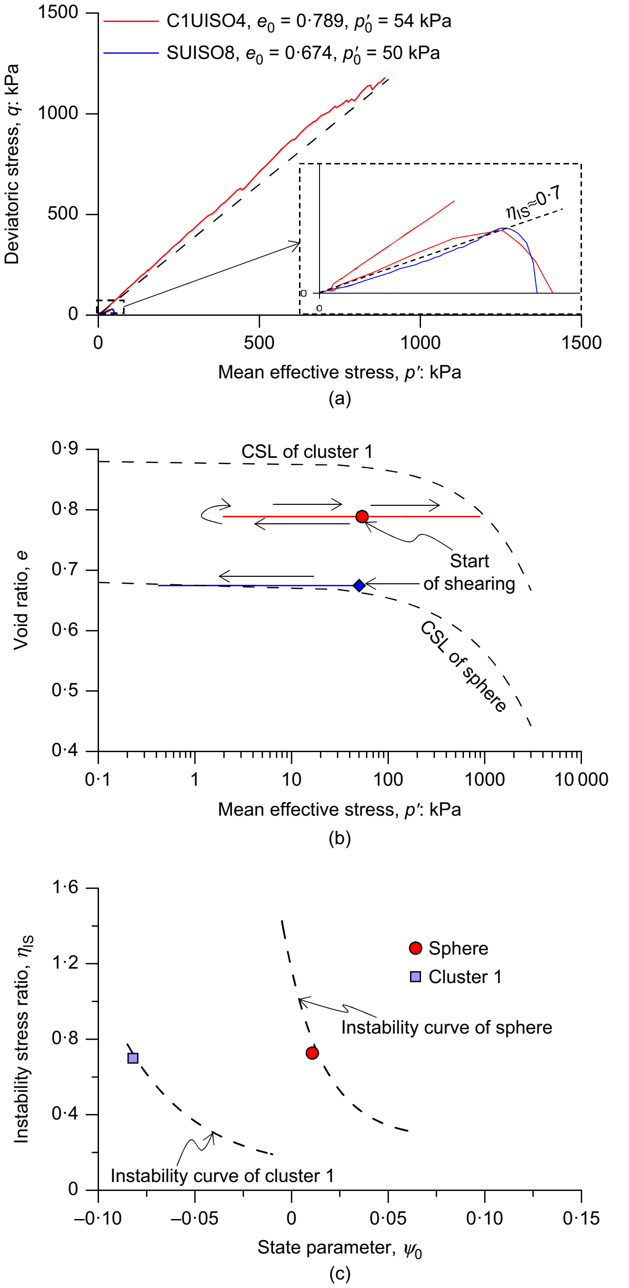

Fig. 20. Comparison of the behaviour of cluster 1 and sphere at a similar η_{IS} in (a) q–p', (b) e–p' and (c) η_{IS}–ψ_0 spaces

for Toyoura sand from Tang & Yang (2019) and Huang *et al.* (2014). Among others, they identified interparticle friction and interpretation of CS as the reason for such difference. In the authors' view, the output of a calibrated DEM model for Toyoura sand cannot be generally assumed the same for all uniform soils with rounded particles, particularly for this qualitative study, which did not have the same PSD and calibrated model parameter for a particular soil. Among others, the major differences – for example, calibrated/qualitative, particle size, PSD, contact model and so on – are outlined in Table 6.

TRIGGERING OF INSTABILITY

Yang (2002) proposed an exponential relation between η_{IS} and ψ_0 relations; however, the relation is material dependent. To overcome this, many studies normalised η_{IS} by M – that is, η_{IS}/M, but the η_{IS}/M–ψ_0 relation is still material dependent. Toyoura sand is subrounded and Merriespruit tailings is angular, but the η_{IS}/M–ψ_0 relation of Toyoura sand is below Merriespruit tailings despite their uniform gradation, see original Fig. 10(a) in the paper by Nguyen *et al.* (2021). Therefore, the relative location of two different η_{IS}/M–ψ_0 curves for two different soils cannot be interpreted as stronger or weaker, as they do not possess any relationship. Despite the authors' efforts, only five out of 16 cluster assemblies showed instability. Interestingly, highly angular particles exhibited static liquefaction even though their initial states were below the CSL line in Fig. 10(a) in the paper by Nguyen *et al.* (2021). To demonstrate this, the authors will be using two simulations from the original publication (Nguyen *et al.*, 2021).

The cluster assembly (C1UISO4) with a state below the CSL – that is, negative ψ_0 – during undrained loading showed initial contraction, then exhibited phase transformation to turn right to exhibit very strong dilation (Figs 20(a) and 20(b)). However, an assembly of spheres (SUISO8) was located slightly above the CSL – that is, positive ψ_0 – and exhibited contractive/complete liquefaction. Both of these assemblies had almost the same η_{IS}. However, due to their ψ_0 and exhibiting limited flow as opposed to flow behaviour, the η_{IS}–ψ_0 curve for angular particles locates below the spherical particle curve. For this reason, the authors deliberately reported 'the η_{IS}/M–ψ_0 relations move downward', instead of suggesting it was stronger.

Finally, the observed behaviour is consistent with the CSSM framework as demonstrated above, which has been further validated with the constitutive model in the paper by Nguyen *et al.* (2020).

REFERENCES

Huang, X., O'Sullivan, C., Hanley, K. & Kwok, C. (2014). Discrete-element method analysis of the state parameter. *Géotechnique* **64**, No. 12, 954–965, https://doi.org/10.1680/geot.14.P.013.

Jefferies, M. & Been, K. (2006). *Soil liquefaction: a critical state approach*. London, UK: Taylor & Francis.

Krumbein, W. C. & Sloss, L. L. (1963). *Stratigraphy and sedimentation*. San Francisco, CA, USA: Freeman and Company.

Li, X. S. & Dafalias, Y. F. (2000). Dilatancy for cohesionless soils. *Géotechnique* **50**, No. 4, 449–460, https://doi.org/10.1680/geot.2000.50.4.449.

Li, X. S. & Wang, Y. (1998). Linear representation of steady-state line for sand. *J. Geotech. Geoenviron. Engng* **124**, No. 12, 1215–1217.

Liu, X. & Yang, J. (2018). Shear wave velocity in sand: effect of grain shape. *Géotechnique* **68**, No. 8, 742–748, https://doi.org/10.1680/jgeot.17.T.011.

Nguyen, H. B. K., Rahman, M. M. & Fourie, A. B. (2020). Effect of particle shape on constitutive relation: DEM study. *J. Geotech. Geoenviron. Engng* **146**, No. 7, 04020058.

Nguyen, H. B. K., Rahman, M. M. & Fourie, A. B. (2021). How particle shape affects the critical state, triggering of instability and dilatancy of granular materials – results from a DEM study. *Géotechnique* **71**, No. 9, 749–764, https://doi.org/10.1680/jgeot.18.P.211.

Rabbi, A. T. M. Z., Rahman, M. M. & Cameron, D. A. (2019). The relation between the state indices and the characteristic features of undrained behaviour of silty sand. *Soils Found.* **59**, No. 4, 801–813.

Rahman, M. M. & Sitharam, T. G. (2020). Cyclic liquefaction screening of sand with non-plastic fines: critical state approach. *Geosci. Front.* **11**, No. 2, 429–438.

Rahman, M. M., Lo, S. R. & Baki, M. A. L. (2011). Equivalent granular state parameter and undrained behaviour of sand-fines mixtures. *Acta Geotech.* **6**, No. 4, 183–194.

Rahman, M. M., Lo, S. C. R. & Dafalias, Y. F. (2014). Modelling the static liquefaction of sand with low-plasticity fines.

Géotechnique **64**, No. 11, 881–894, https://doi.org/10.1680/geot.14.P.079.

Rahman, M. M., Nguyen, H. B. K., Fourie, A. B. & Kuhn, M. R. (2021). Critical state soil mechanics for cyclic liquefaction and postliquefaction behavior: DEM study. *J. Geotech. Geoenviron. Engng* **147**, No. 2, 04020166.

Reid, D., Fourie, A., Ayala, J. L., Dickinson, S., Ochoa-Cornejo, F., Fanni, R., Garfias, J., Fonseca, A. V. D., Ghafghazi, M., Ovalle, C., Riemer, M., Rismanchian, A., Olivera, R. & Suazo, G. (2021). Results of a critical state line testing round robin programme. *Géotechnique* **71**, No. 7, 616–630, https://doi.org/10.1680/jgeot.19.P.373.

Tang, X. & Yang, J. (2019). *Effects of gradation and particle shape on wave propagation in granular material, Research Report*. Department of Civil Engineering, The University of Hong Kong, Hong Kong, China.

Verdugo, R. & Ishihara, K. (1996). The steady state of sandy soils. *Soils Founds* **36**, No. 2, 81–91.

Wei, L. M. & Yang, J. (2014). On the role of grain shape in static liquefaction of sand–fines mixtures. *Géotechnique* **64**, No. 9, 740–745, https://doi.org/10.1680/geot.14.T.013.

Wood, D. M., Belkheir, K. & Liu, D. F. (1994). Strain softening and state parameter for sand modeling. *Géotechnique* **44**, No. 2, 335–339, https://doi.org/10.1680/geot.1994.44.2.335.

Yang, J. (2002). Non-uniqueness of flow liquefaction line for loose sand. *Géotechnique* **52**, No. 10, 757–760, https://doi.org/10.1680/geot.2002.52.10.757.

Yang, J. & Li, X. S. (2004). State-dependent strength of sands from the perspective of unified modeling. *J. Geotech. Geoenviron. Eng.* **130**, No. 2, 186–198.

Yang, J. & Luo, X. D. (2015). Exploring the relationship between critical state and particle shape for granular materials. *J. Mech. Phys. Solids* **84**, Supplement C, 196–213.

Yang, J. & Wei, L. M. (2012). Collapse of loose sand with the addition of fines: the role of particle shape. *Géotechnique* **62**, No. 12, 1111–1125, https://doi.org/10.1680/geot.11.P.062.